phys. stat. sol. (a) 80, 305 (1983)

Subject classification: 1.3; 9; 21; 21.6

Materials Science Centre, Indian Institute of Technology, Kharagpur[1])

On the Variation of Interface Composition around a Dissolving Precipitate

By

S. K. PABI

An analysis of the solute transfer from precipitates of time invariant composition shows that the flux across the interface during the solution treatment is proportional to $(C_E^2 - C_S^2)$, where C_S and C_E are, respectively, the local and equilibrium compositions of the matrix at the interface. Apart from a numerical analysis, a close-form expression developed can also define satisfactorily the variation of C_S for the precipitate plates with the solution time. The C_S approaches C_E asymptotically at a finite rate depending primarily on the activation energy for the atomic jump across the interface, an accommodation coefficient, and the diffusivity of the solute in the matrix. A deviation of C_S from C_E can be observed for coherent as well as high melting incoherent precipitates. A simple model for the mass transfer proposed can explain several characteristic features of the dissolution. The theory is applied to the solution data for the Al–Si and Al–Ag alloys.

Eine Analyse des Übergangs des gelösten Stoffes von Ausscheidungen mit zeitunabhängiger Zusammensetzung zeigt, daß der Fluß über die Grenzfläche während des Lösungsvorganges proportional zu $(C_E^2 - C_S^2)$ ist, wobei C_S und C_E die lokalen bzw. Gleichgewichtszusammensetzungen der Matrix an der Grenzfläche darstellen. Außer einer numerischen Analyse wird ein geschlossener Ausdruck abgeleitet, der die Variation von C_S für Ausscheidungsplättchen mit der Lösungszeit befriedigend definiert. C_S nähert sich C_E asymptotisch mit einer endlichen Rate, die hauptsächlich von der Aktivierungsenergie für die Atomsprünge über die Grenzfläche, einem Anpassungskoeffizienten und dem Diffusionsvermögen des gelösten Stoffes in der Matrix abhängt. Eine Abweichung von C_S von C_E wird für kohärente sowie für hochschmelzende inkohärente Ausscheidungen beobachtet. Mit einem für den Massenausgleich vorgeschlagenen einfachen Modell lassen sich charakteristische Einzelheiten des Lösungsvorgangs erklären. Die Theorie wird auf die Lösungswerte für Al–Si- und Al–Ag-Legierungen angewendet.

1. Introduction

Solution of second phase particles in solids takes place by mass transfer across mobile interfaces. Quantitative treatments of the problem usually assume a steady state composition at the interphase interface right from the inception of the homogenization [1 to 7]. Numerous experimental evidences, however, suggest that the local equilibrium at the interface may [8] or may not [9 to 13] exist. For growth of the crystals from solutions, Brice [14] has derived the rate equations for several possible modes of variation of the interface composition. But these formulations are not directly applicable to the solid–solid transformations, for which the appropriate rate equations are not known a priori.

A few theoretical investigations reported on the interface controlled solution kinetics in solids [10, 15, 16] have made various simplifying assumptions, the common one essentially being a time-invariant second phase composition. In a comprehensive analytical treatment for spherical precipitates dissolving in a finite matrix Nolfi et al. [10] have characterized the flux across the interface as proportional to $(C_S - C_E)$,

[1]) Kharagpur 721302, India.

where C_S and C_E are the actual and equilibrium solute content, respectively, in the matrix at the interface. For solution of an isolated spherical particle in an infinite matrix Aaron and Kotler [15] have proposed a numerical treatment based on a uniform detachment mechanism, whereby the interface growth velocity is expressed as $V = -k_0(C_E - C_S)$; k_0 is a rate constant. The computation reveals that the interface reaction mechanism will have no sensible effect for $k_0 > 10^{-6}$ m/s, and for $k_0 < 10^{-9}$ m/s the particle is effectively insoluble due to the extremely sluggish kinetics. The interface migration can have a remarkable effect on solution kinetics [5]. Nolfi and Aaron have ignored this factor, whereas Lyubov and coworkers [16] have taken it into account and illustrated the retardation of solution kinetics due to the surface phenomenon in the final stage of the process. The formulation assumes $V = -k_1(C_E - C_S)$, where $k_1 = k_0 R_0/D$, R_0 is the starting radius of the precipitate and D is the diffusion coefficient of the solute in the matrix. Lyubov et al. have noted the remarkable influence of the surface process when $k_1 < 10^{-1}$. If $k_1 < 10^{-5}$, the precipitate is practically insoluble and, when $k_1 \geqq 10^2$ the process of dissolution could be taken as being limited by diffusion. The basis of the kinetic equations for the variation of C_S used in the above models is not quite well founded. The present investigation attempts to derive the closed form expressions for the flux across the singular interfaces and for the variation of C_S with solution time.

2. Theoretical

The schematic phase diagram of a binary system A–B has been illustrated in Fig. 1. The composition[2]) of the solute rich β phase C_B does not vary with temperature. An alloy of composition C_A equilibrated at the temperature T_1 would have β particles embedded in the matrix phase α of composition C_M. If the alloy is then up-quenched to a temperature T the system inclines to attend the new equilibrium condition corresponding to T with consequent dissolution of β. Concurrently, the composition of the matrix at the α/β interface moves towards C_E and the concentration–distance profile across a decaying β particle has been displayed schematically in Fig. 2. The zero mass transfer plane is the plane of symmetry of the precipitate.

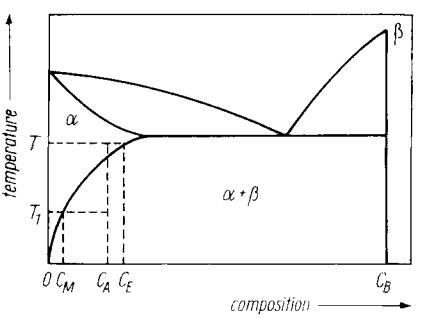

Fig. 1

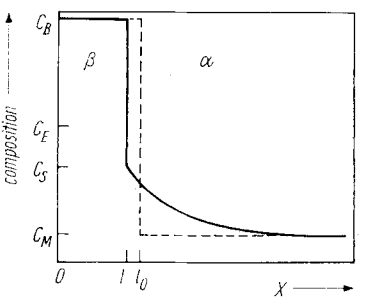

Fig. 2

Fig. 1. A binary phase diagram showing limited solubility of B in A and the β phase of invariant composition (schematic)

Fig. 2. Solute concentration profile around a β-particle at the solution temperature T. The dashed lines illustrate the condition at $t = 0$, and the full line at some $t > 0$. The origin coincides with the zero mass transfer plane in the precipitate

[2]) The compositions are expressed in model fraction B, unless otherwise stated.

2.1 The driving force

At the dissolution temperature the A and B atoms would be redistributed between the α and β phases. When equilibrium is attained, the chemical potential of every constituent in each of the phases would be equal. If the activity coefficients of A and B at T remain constant in α over the composition range C to C_E[3]) the net free energy change due to the solution of one mole of β having a general formula A_mB_n in the α-phase of composition C can be written as [17]

$$-\Delta G_v' = RT\left(n \ln \frac{C}{C_E} + m \ln \frac{1-C}{1-C_E}\right), \tag{1}$$

where n and m are the number of ions of A and B formed from one molecule of β. If the solution is dilute, the second term in the parenthesis can be conveniently neglected[4]) and the total free energy change associated with the transfer of one mole of B from β to α is given by

$$-\Delta G_v = RT \ln \frac{C}{C_E}. \tag{2}$$

Further simplification of (2) in a manner analogous to Nolfi et al. [10] and Brice [14] by writing $\ln (C/C_E) \approx (C - C_E)/C_E$ is not attempted here, since the truncation error involved is of the order of $(C_E - C)/2C_E$ which may not be negligible at all.

2.2 Flux across the interface

Let the β phase have a planar geometry which is presumably retained during solution treatment[5]) and naturally, the change in the interfacial energy term can be ignored. The free energy change due to the redistribution of A atoms is usually negligible (cf. Section 2.1) and hence only the flux of solute atoms would be taken into consideration which is assumed to occur independent of solvent atom redistribution. The α/β interface is thought to be sharp and the transport of B atoms is believed to be a single atom process. Experimental evidences indicate that the dissolution of coherent as well as incoherent precipitates takes place by a ledge mechanism [19 to 21] possibly

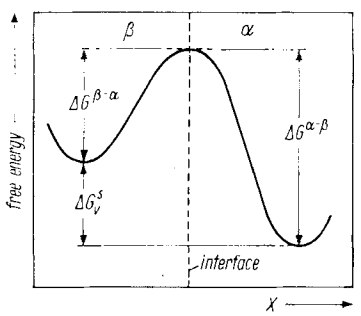

Fig. 3. Schematic illustration of the activation energy barrier and the free energy change accompanied with the movement of the B atoms across the α/β interface

[3]) This assumption imposes less constraint than that implied for a Henrian solution because in the latter case the activity coefficient must remain constant over the composition range 0 to C_E.

[4]) For instance, in the dissolution of an AB-type compound if $C = 0.0001$ and $C_E = 0.05$, this approximation would introduce an error of $\approx 0.6\%$ in the estimated value of $\Delta G_v'$.

[5]) Several investigations [8, 9, 13] on the dissolution of planar precipitates have not reported any perturbation of the planar interface on a microscopic scale. In an experiment on the dissolution of β-brass plates in α-brass, however, Heckel et al. [18] observed that prolonged holding at the solution temperature can make the interface slightly irregular primarily due to the surface tension effects of α-phase boundaries.

by transfer of atoms at the kink of the ledges (cf. Section 4.1). For the ensuing analysis it may be postulated that a steady state distribution of these kinks or similar active sites on the interface would be present or attained in a negligibly short period at the solution temperature.

The energy relation for the thermally activated jump of B atoms across the interface at the solution temperature is depicted schematically in Fig. 3. The number of atoms going from β to α per unit area of the interface per unit time is

$$\frac{C_B N_\beta p_\beta \omega_\beta Q_\alpha}{J_\beta} \exp\left(-\frac{\Delta G^{\beta-\alpha}}{RT}\right),$$

where N_β is the number of atoms per unit area of β at the interface, ω_β the vibration frequency in β of the order of the Debye frequency, p_β the probability that a vibration in the second phase is in correct direction, J_β the number of jumps required to cross the interface from β to α, Q_α the accommodation coefficient of α at the interface, i.e. the fraction of sites on the surface of α at the interface at which B atoms crossing the interface can be accommodated, R the universal gas constant, $\Delta G^{\beta-\alpha}$ the activation energy barrier for the B atoms to cross the interface from β to α in units of kJ/mol. The number of B atoms crossing the interface in the reverse direction, i.e. from α to β per unit area per unit time is

$$\frac{C_S N_\alpha p_\alpha \omega_\alpha Q_\beta}{J_\alpha} \exp\left(-\frac{\Delta G^{\alpha-\beta}}{RT}\right),$$

where the symbols have similar meaning and correspond to the other phase.

The net rate of transfer of the B atoms from the precipitate to the matrix

$$\delta = \frac{N_\beta p_\beta \omega_\beta Q_\alpha}{J_\beta} \exp\left(-\frac{\Delta G^{\beta-\alpha}}{RT}\right)\left[C_B - Y C_S \exp\left(-\frac{\Delta G_v^s}{RT}\right)\right], \tag{3}$$

where

$$Y = \frac{N_\alpha p_\alpha \omega_\alpha Q_\beta J_\beta}{N_\beta p_\beta \omega_\beta Q_\alpha J_\alpha} \tag{4}$$

and ΔG_v^s is the change in free energy due to the transport of one mole of B from the interface of the β phase to the interface of α having a composition C_S. If the strain energy and the gradient free energy terms are neglected for simplicity[6]), $\Delta G_v^s = \Delta G_v$ and hence, substitution of equation (2) in (3) yields

$$\delta = \frac{N_\beta p_\beta \omega_\beta Q_\alpha}{J_\beta} \exp\left(-\frac{\Delta G^{\beta-\alpha}}{RT}\right)\left[C_B - Y \frac{C_S^2}{C_E}\right]. \tag{5}$$

[6]) An estimate of the maximum strain energy associated with the transformation can be obtained by following Swartz [22] from the difference in the molar volume of the diffusing species in the two phases involved through the application of the elasticity theorem. For dissolution of Fe_3C in ferrite [12] the strain energy contribution was only about 0.1% of the driving force. The local free energy per molecule in a region with spatial variation in composition depends not only on the local composition but also on the composition of the immediate environment. The gradient term of the free energy in the present case should be proportional to the square of the concentration gradient in the matrix adjacent to the interface, the proportionality constant being related to the gradient of free energy with composition [23]. Both of these energy terms increase the chemical potential of B atoms at the interface in α and, thereby, diminish the driving force of the transformation and retard the rate of approach to the equilibrium condition at the interface.

When the local equilibrium at the interface is attained, the chemical potential of the B atoms adjacent to either side of the interface becomes equal and, in absence of a chemical potential gradient the net mass transfer across the interface would be zero, i.e.,

$$\delta = 0 \quad \text{at} \quad C_S = C_E \,. \tag{6}$$

When $T > 0$, (5) subjected to condition (6) gives

$$C_B = Y C_E \tag{7}$$

provided J_β is finite and $Q_\alpha \neq 0$. Equation (5) in conjunction with (4) and (7) can now be rewritten as

$$\delta = K N_\alpha \frac{\Delta^2 C}{C_E}, \tag{8}$$

where

$$K = \frac{p_\alpha \omega_\alpha Q_\beta}{J_\alpha} \exp\left(-\frac{\Delta G^{\beta-\alpha}}{RT}\right) \tag{9}$$

and

$$\Delta^2 C = C_E^2 - C_S^2 \,. \tag{10}$$

Equations (8) through (10) suggest that the flux across the interface at any instant is proportional to the difference of the squares of the equilibrium and actual compositions of the matrix at the interface and the proportionality constant should increase exponentially with the solution temperature.

2.3 Variation of interphase composition

At any instant t at the solution temperature dC_S/dt would depend on the flux across the interface and the flux in α from the interface to the matrix. If ϱ is the spacing between the adjacent planes in α parallel to the habit plane and l is the position of the interface along the X coordinate (cf. Fig. 2), (8) together with Fick's first law yields

$$\frac{dC_S}{dt} = K \frac{C_E^2 - C_S^2}{C_E} - \frac{D}{\varrho}\left(\frac{\partial c}{\partial X}\right)_{X=l^+}, \tag{11}$$

where the last term represents the gradient at l towards increasing l.

For an array of β plates of uniform initial thickness $2l_0$ stacked at equal interval $2L$ in α, C_S may be evaluated from the solution of (11) coupled with the following conditions:

$$\frac{\partial c}{\partial t} = D \frac{\partial^2 c}{\partial X^2}; \qquad l \leqq X \leqq L \,, \tag{12}$$

$$C = C_M \,; \qquad l_0 \leqq X \leqq L \,, \qquad t = 0 \,, \tag{13}$$

$$C = C_S \,; \qquad X = l \,, \qquad t < 0 \,, \tag{14}$$

$$\left(\frac{\partial c}{\partial X}\right) = 0 \,, \qquad X = L \,, \qquad t < 0 \,. \tag{15}$$

$$(C_B - C_S)\frac{dl}{dt} = D\left(\frac{\partial c}{\partial X}\right)_{X=l^+}. \tag{16}$$

Rigorous numerical solution of (11) through (16) by a finite difference scheme after applying a variable grid space transformation [24] in a manner similar to that of Tanzilli and Heckel [6] is extremely time consuming and inconvenient because (i)

large error is associated in the calculation of the last term of (11) unless the grid spacing is of the order of ϱ and as a result (ii) Δt must very small to avoid computational instability.

However, for calculation of the dissolution kinetics of planar precipitates it may be reasonable to assume that the composition gradients are linear [1, 5, 25] and if C_A is small, the impingement of the diffusion fields of adjacent precipitates would have negligible influence on the dissolution kinetics. Under this condition it may be readily shown that

$$\frac{dC_S}{dt} = K\frac{C_E^2 - C_S^2}{C_E} - \frac{1}{2\varrho}\left(\frac{D}{t}\right)^{1/2}(C_S - C_M)\left[\frac{C_B - C_S}{C_B - C_M}\right]^{1/2}; \quad C_S \leqq C_E . \tag{17}$$

Equation (17) has been solved numerically by the Runge-Kutta method [26] with initial condition $C_S = C_M$ at $t = 0$, and prolonged computation (about 90 min for each set) is required to avoid computational instability.

For many practical homogenization problems $C_B \gg C_E$ and (17) may be simplified by considering $[(C_B - C_S)/(C_B - C_M)]^{1/2} \approx 1$, and reducing the composition scale by a multiplying factor $1/C_E$. Thus,

$$\frac{d\bar{C}_S}{dt} = K_1\theta(1 - \bar{C}_S^2) - (\bar{C}_S - \bar{C}_M); \qquad \bar{C}_S \leqq 1 , \tag{18}$$

where $K_1 = 2K\varrho^2/D$, $\theta = \sqrt{Dt}/\varrho$, the bar indicates the rationalized compositions and essentially $\bar{C}_E = 1$. If $\bar{C}_S$ increases to C_E (in the limit) after one second or more, $K_1 \ll 1$. Expressing $\bar{C}_S$ as

$$\bar{C}_S = C_0K_1^0 + C_1K_1^1 + C_2K_1^2 + C_3K_1^3 + \ldots \tag{19}$$

and neglecting K_1^2 and higher order terms, an approximate solution of (18) by regular perturbation method [27] may be written as

$$\bar{C}_S = \bar{C}_M + \frac{2K\varrho^2}{D}(1 - \bar{C}_M^2)(e^{-\theta} + \theta - 1); \qquad \bar{C}_S \leqq 1) . \tag{20}$$

3. Results

3.1 Comparison between the theoretical solutions

The numerical solution of (11) by the finite difference scheme has not been complete because it would take several days on an EC1030 computer to work out a C_S versus t plot. However, there is a definite indication that the predictions by this scheme agrees well with the numerical solution of (17). Unless the incremental time Δt is very small, the solution of (17) becomes unstable, because C_S often augments slowly as a result of two fairly fast processes, namely, the solute transfer from the precipitate to the matrix and the diffusion flux in α from the interface into the matrix.

Table 1

Input parameter values for some hypothetical systems

system No.	C_P	C_E	C_M	C_A	D ($\mu m^2/s$)	ϱ (nm)	K (s^{-1})
I	0.995	0.0082	0.0023	0.0056	0.136	0.2333	1000
II	0.995	0.0082	0.0023	0.0056	0.0136	0.2333	100
III	0.995	0.0082	0.0023	0.0023	0.0136	0.2833	10
IV	0.6	0.02855	0.01997	0.0325	0.01	0.2333	100
V	0.6	0.02855	0.01997	0.0325	0.01	0.2333	10
VI	0.6	0.02855	0.01997	0.0325	0.01	0.2333	1

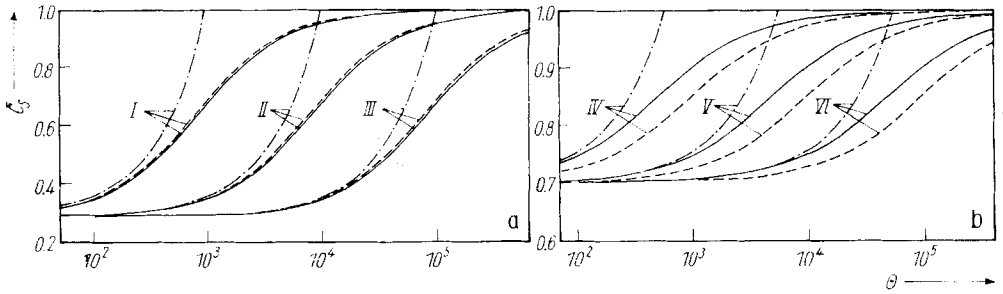

Fig. 4. Variation of $\bar{C}_S$ with θ for the systems a) I, II, and III and b) IV, V, and VI predicted by (17) (———), (20), (—·—), and (22) (— — —)

Fig. 4 displays the time evolution of $\bar{C}_S$ obtained from (17) and (20) for various sets of input parameter values enlisted in Table 1. The compositions and diffusivities for systems I to III are typical for Al–Si alloys [13] and those for IV to VI correspond to the Al–Ag system [9]. It appears that if the K values are kept constant, curves obtained from (17) or (20) are isokinetic. The predictions of (20) differ appreciably from the numerical solution of (17); the deviation widens with the increase of $\bar{C}_S$, because (20) ignores K_1^2 and higher-order terms, which may not justified for larger values of θ.

Equation (20) may be modified intuitively as

$$\bar{C}_S = \bar{C}_M + \frac{2K\varrho^2}{D}(1 - \bar{C}_S^2)(1 - \bar{C}_M^2)(e^{-\theta} + \theta - 1) . \tag{21}$$

Often $\theta \gg 1$, e.g., when $t = 1$ s in system I, $\theta = 1611$. There (21) can be symplified as

$$\bar{C}_S = \bar{C}_M + \frac{2K\varrho^2\theta}{D}(1 - \bar{C}_S^2)(1 - \bar{C}_M^2) . \tag{22}$$

Fig. 4a shows that the variation of $\bar{C}_S$ obtained from (22) is in conspicuous agreement with the numerical solution of (17). The agreement is somewhat less pronounced for the systems IV through VI (Fig. 4b). Nevertheless, it appears that (22) is a closed form, approximate solution (17).

3.2 Application to the experimental data

Detailed microprobe analyses have revealed that the interface composition of the dissolving precipitates deviates from equilibrium in Al–Ag [9] and Al–Si [13] systems. The C_E for these systems was noted from the data compiled by Mondolfo [28] and the dissolution data reporting C_S values greater than this C_E have been rejected from the ensuing analysis. The precipitates in Al–Ag alloys form with the orientation relationship [29]

$$(001)_\gamma \,||\, (111)_{Al}; \qquad [110]_\gamma \,||\, [110]_{Al} ,$$

whereas for precipitation of Si in Al preference for several orientation relationships has been observed [30]. Assuming $(111)_{Al}$ is the habit plane, $\varrho = 0.2333$ nm. The experimental data [9, 13] along with the reported D values have been fitted to (22) yield the values of K. Fig. 5 presents the plot of ln K against the reciprocal of the solution temperature for the Al–Ag and Al–Si alloys. The data show a wide scatter, particularly for the Al–Si system and the least-squares straight line fits through these points have been illustrated. Several factors can be responsible for the observed

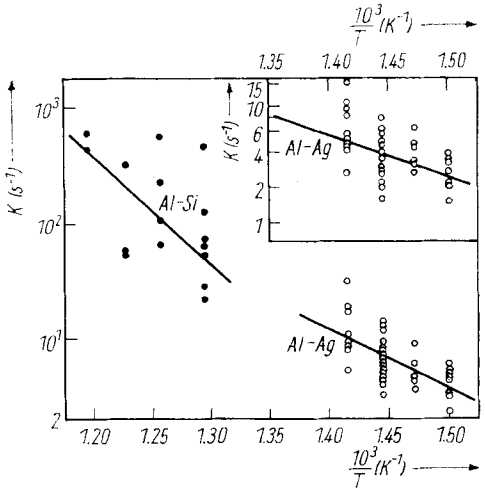

Fig. 5. An Arrhenius plot of K computed from the dissolution data of the γ-precipitates (○) and Si-precipitates (●) in Al–Ag [9] and Al–Si [13] alloys, respectively. The K values in the inserted plot are obtained through the numerical solution of (17) and in the rest of the figure through (22)

diversity in the K values. The accommodation coefficient can vary widely from one precipitate to another with time and ϱ may be different for different particles. The main possible sources of experimental error are as follows:

(i) The precipitate plates were often not vertical to the polished surface and the asymmetry in the field boundary condition between the two sides of an inclined precipitate cannot be corrected for by any simple means.

(ii) Limited resolution of an electron microprobe analyzer induces to apply some regression scheme to obtain C_S. The basic equations used in this analysis [9, 13] presume either a time invariant C_S or dC_S/dt proportional to $(C_E - C_S)$, and a closed form expression for the concentration profile with the boundary condition (22) is not available as yet. This factor along with the inherent error in any regression scheme can be quite important, because the composition gradient near the interface is usually steep.

(iii) Limited precision of the concentration values measured by a microprobe analyzer.

The total limit of uncertainty in the experimental value of C_S reported [9, 13] cannot be ascertained at the moment. It is apparent from Fig. 4 that if $\bar{C}_S < 0.9$, a small error in the estimation of $\bar{C}_S$ would introduce a large error in K. For a fairly accurate estimation of K, the t for $\bar{C}_S < 0.8$ should be measured, and this condition has not been fulfilled by the experimental data [9, 13].

If the pre-exponential terms in (9) do not vary with time and temperature of solution treatment, the slope of the straight lines in Fig. 5 would yield the value of $\Delta G^{\beta-\alpha}$, and from the intercept the accommodation coefficient Q_β can be estimated in the following way. Taking the elastic constant for Al-rich matrix $E = 40$ GN/m^2, $\varrho = 0.2333$ nm, and the atomic mass $= 1.79 \times 10^{-25}$ kg [28], ω_α can be calculated [31] as $\approx 1.15 \times 10^{12}$ s^{-1}. Assuming p_α for cubic crystal equal to $\frac{1}{6}$ and $J_\alpha = 1$, Q_β is evaluated. The $\Delta G^{\beta-\alpha}$ and Q_β calculated from the data on Al–Ag [9] and Al–Si [13] systems through the estimation of K by (22) are given in Table 2. Since a small uncertainty in the afore-said slope induces a large error in Q_β, only the order of magnitude of Q_β has any practical relevance.

The experimental data can be fitted to the numerical solution of (17), since the rate of change of C_S is almost isokinetic for a wide variation of K (cf. Fig. 4). The values of K obtained in this way for the Al–Si system were practically the same as

that from (22) reported above and those for Al–Ag alloys have been inserted in Fig. 5. The $\Delta G^{\beta-\alpha}$ and Q_β calculated from these K values are given in Table 2. From Table 2

Table 2
Results of analysis of the experimental data in [9] and [13]

system	dissolving precipitate	from (22)		from numerical soln. of (17)	
		$\Delta G^{\beta-\alpha}$ (kJ/mol)	Q_β	ΔG (kJ/mol)	Q_β
Al–Ag	Ag_2Al	96	8×10^{-4}	68	2.8×10^{-6}
Al–Si	Si	176	25	178	193

it is evident that a small systematic error in the calculation of K can substantially alter the magnitude of $\Delta G^{\beta-\alpha}$ and Q_β estimated.

4. Discussion

4.1 A model for mass transfer from the dissolving precipitates

Consider the initiation of solute transfer from the β particle in Fig. 6, which is bound by singular incoherent interfaces and surrounded by α. A thermally activated jump of single atoms (represented by the small cubes) across the α/β interface can take place from three kinds of sites, namely, i, j, k. The transfer from i-type sites would be free from any nucleation barrier and the single ledge can propagate readily along the cube surfaces PQRS, PQUT, and PSWT (cf. Fig. 6) without any nucleation barrier. The ledge front would be nearly parallel to the diagonals QS, QT, and ST, respectively, if the atoms detach at random. The impingement of the ledges propagating from several nucleation sites on any interfacial plane would result in dislocation loops enclosed between interfacial partials which would eventually collapse and disappear.

On the other hand, if the interfacial energy is isotropic, the activation barrier for the ledge nucleation from the k-type site is eight times that for the j-type. The kink on a single ledge at g-type site can propagate spontaneously along the edge RS, then circumscribe the precipitate edges and eventually disappear. The ledge created in this way can move towards the centre of the precipitate and/or increase its height to form a multi-atomic layered ledge by nucleation and propagation of fresh kinks. The ledge front, however, can meet some suitably oriented dislocation in the precipitate (e.g. an edge dislocation with Burgers vector perpendicular to ledge front), following which the ledge front would advance in the radial direction along the interface spontaneously. On the contrary, progressive removal of the atoms in β from the k-type sites can occur only through fresh nucleation of kinks, which is quite unfavourable. Thus, if the driving force is not infinitesimal, solution of the precipitates with incoherent interfaces (or with boundaries consisting of regions in forced elastic co-

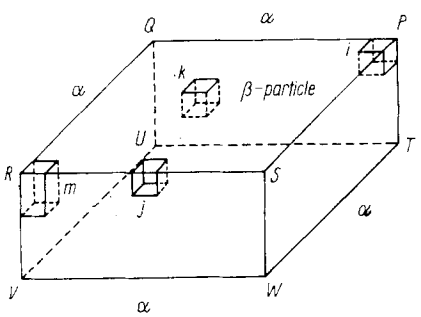

Fig. 6. Schematic diagram of a β particle surrounded by the α-matrix (see text)

herence separated by regions of misfit) would usually take place by nucleation of closely spaced singular as well as multi-atomic layered ledges at the edge of the precipitate. The conjecture agrees fully with the careful electron microscopic observations of the dissolution ledge in the $\theta(CuAl_2)$ and $\beta(Mg_2Si)$ precipitates [21] formed in Al–Cu and Al–Mg–Si alloys, respectively.

If some of the interfaces of the precipitate are coherent, viz. the surfaces PQRS and TUVW in Fig. 6, and the rest of the boundary is incoherent, removal of single atoms from any of the sites i, j, k can lead to forbidden packing [32]. In that case a ledge can nucleate by removal of a "pill-box" consisting of several atoms (cf. site m in Fig. 6) with stable interfacial configuration. The ledge front can migrate like a single ledge along the incoherent interfaces. On the coherent faces, however, the multiatomic layered ledge would move inwards and/or increase its height, in a way similar to that for incoherent precipitates. In brief, the criteria for stability of the interfacial configuration for the coherent interface usually precludes the possibility of formation of single ledges and favours the multi-atomic layered ledge or the macroscopic ledge (i.e. a combination of several multi-atomic layered ledges associated with a Shockley partial) nucleation. The electron microscopic observations support this view. γ'-plates in Al–Ag alloy dissolve by gradual removal of successive layers of the precipitate by contraction and elimination of interfacial partials [19]. The θ' plates in an Al–Cu alloy dissolve by nucleation of the multi-atomic layered ledge at the edge of the plates; the ledges migrate inwards ultimately forming loops which quickly collapse and disappear [20]. Weatherly [21] has specifically noted the complete absence of the single ledges on dissolving θ' plates.

It is obvious that the fraction of interfacial sites, Q, at which mass transfer can take place should have a value close to unity for the incoherent interfaces due to the ease of the formation of single ledges on these interfaces. For coherent interfaces, on the contrary, Q is expected to be much smaller in magnitude.

4.2 Dissolution mechanism of the second phase

In Al–Si alloy because of the large mismatch between the precipitate and the matrix, coherency is lost in a quite early stage of precipitation [28]. Solution of the large Si-precipitates selected [13] should, therefore, take place by mass transfer across incoherent interfaces. The estimated Q_β for this system supports this view, although caution is warranted in the prediction of the solution mechanism from Q_β and $\Delta G^{\beta-\alpha}$ due to the errors in the estimation of these parameters (cf. Section 3.3). $\Delta G^{\beta-\alpha}$ for the Si precipitates (cf. Table 2) is greater than the reported [13, 28] activation energy for the volume diffusion of Si in Al (127 kJ/mol), and is about 40%, 50%, and 75% of the activation energies for the volume self-diffusion of Si [33], the surface self diffusion of Si [34], and the grain boundary impurity diffusion in Si [35], respectively. Nevertheless, the present theoretical analysis clearly shows in principle that an observed deviation of C_S from C_E need not necessarily be attributed to some marked crystallographically related features of the interface, and an incoherent precipitate can dissolve with a notable nonequilibrium C_S, if the $\Delta G^{\beta-\alpha}$ is large.

Laird and Aaronson [36] have shown that the broad faces of γ-precipitates in the Al–Ag alloy have dislocation-type boundaries composed of the complex array of the Shockley partials. The dislocations are arranged in the step configuration like built-in ledges to avoid forbidden packing. The solution of the γ-precipitates should, therefore, be associated with $Q_\beta \ll 1$ (cf. Section 4.1) — a fact well in accordance with the results of the present experimental data analysis (cf. Table 2). The well-defined orientation relationship of the γ-precipitates should bring about an arrow spectrum of $\Delta G^{\beta-\alpha}$. However, $\Delta G^{\beta-\alpha}$ of the Ag_2Al precipitates is less than half that for the Si

precipitates (cf. Section 3.3) and is of the order of the activation energy for the grain boundary diffusion in Ag_2Al [37]. The solute transfer from a compound second phase, unlike from an elemental precipitate, can go through several intermediate steps. For instance, in a similar problem of the detoriation of silicate glasses in aqueous media, Paul and coworkers [38, 39] have found that the mass transfer from the glass must be preceded by a rate limiting step of hydration of the constituent oxides. $\Delta G^{\beta-\alpha}$ for the compound precipitates, viz. Ag_2Al, can correspond to the similar rate limiting steps.

In general, (8) and (22) point out that irrespective of the crystallographic nature of the interface, C_S approaches C_E asymptotically at a finite rate depending primarily on $\Delta G^{\beta-\alpha}$, Q_β, and D. The kinetics for any particular combination of C_E, C_M, D, and ϱ can be represented by a single curve of $\bar{C}_S$ versus $K\theta$ (cf. Fig. 4). Whether the deviation from the local equilibrium at the interface would be detectable or not will depend on the precision of measuring $\bar{C}_S$, the smallest t at which $\bar{C}_S$ is measured, the magnitude of D, and, of course, how small K is. Further, (9) indicates that the sluggish approach to the local equilibrium at the interface can be noticed if (i) Q_β is small, which probably holds good for the coherent and semicoherent precipitates and (ii) $\Delta G^{\beta-\alpha}$ is large. Solution of a high-melting second phase (i.e., a phase with high internal bond strength) always has a fair chance of exhibiting a nonequilibrium value of $\bar{C}_S$.

The transition phases usually have a crystal structure and habit plane which allow them to achieve exceptionally good lattice matching with the matrix [40]. As a result, Q_β for thes precipitates is likely to be several orders of magnitude smaller than that for the final precipitates, although ΔC^2_{max} for both the phases are almost identical. Equations (8) and (9), therefore, suggest that the transition phases should usually dissolve at a slower rate than the respective final precipitates.

Acknowledgements

The author is indebted to Prof. A. S. Gupta and Prof. A. Paul for many stimulating discussions. The technical assistance of Mr. B. P. Mondal and Mr. B. K. Dasgupta is greatly appreciated. Thanks to Dr. Satyajit Banerjee for scrutinizing the manuscript.

References

[1] H. B. Aaron, Metal Sci. J. **2**, 192 (1968).
[2] M. J. Whelan, Metal. Sci. J. **3**, 95 (1969).
[3] S. N. Singh and M. C. Flemings, Trans. TMS-AIME **245**, 1803 (1969).
[4] A. Pasparakis and L. C. Brown, Acta metall. **21**, 1259 (1973).
[5] S. K. Pabi, Acta metall. **27**, 1693 (1969).
[6] R. A. Tanzilli and R. W. Heckel, Trans. TMS-AIME **242**, 2313 (1968).
[7] S. K. Pabi, phys. stat. sol. (a) **51**, 281 (1979).
[8] M. G. Hall and C. W. Howorth, Acta metall. **18**, 331 (1970).
[9] K. Abbott and C. W. Howorth, Acta metall. **21**, 951 (1973).
[10] F. V. Nolfi, jr., P. G. Shewon, and J. S. Foster, Trans. TMS-AIME **245**, 1427 (1969).
[11] F. V. Nolfi, jr., P. G. Shewmon, and J. S. Foster, Metallurg. Trans. **1**, 789 (1970).
[12] F. V. Nolfi, jr., P. G. Shewmon, and J. S. Foster, Metallurg. Trans. **1**, 2291 (1970).
[13] S. K. Pabi, Mater. Sci. Engng. **43**, 151 (1980).
[14] J. C. Brice, J. Crystal Growth **1**, 218 (1967).
[15] H. B. Aaron and G. R. Kotler, Metallurg. Trans. **2**, 393 (1971).
[16] B. Y. Lyubov, F. N. Khazanovich, and V. V. Shevelev, Phys. Met. and Metallography **37**, 47 (1974).
[17] K. Denbigh, The Principles of Chemical Equilibrium, Cambridge University Press, Cambridge 1968.

[18] R. W. Heckel, A. J. Hickel, R. J. Zaehring, and R. A. Tanzilli, Metallurg. Trans. **3**, 2565 (1972).
[19] J. A. Hren and G. Thomas, Trans. TMS-AIME **227**, 308 (1963).
[20] C. Laird and H. I. Aaronson, J. Inst. Metals **96**, 222 (1968).
[21] G. C. Weatherley, Acta metall. **19**, 181 (1971).
[22] J. C. Swartz, Trans. TMS-AIME **239**, 68 (1967).
[23] J. W. Cahn and J. E. Hilliard J. chem. Phys. **28**, 258 (1958).
[24] W. D. Murry and F. Landis, Trans. ASME. Ser. D **81**, 160 (1959).
[25] C. Zener, J. appl. Phys. **20**, 950 (1949).
[26] J. M. McCormick and M. G. Salvadori, Numerical Methods in Fortran, Prentice-Hall of India, New Delhi 1971.
[27] A. H. Nayfeh, Perturbation Methods, John Wiley, New York 1973.
[28] L. F. Mondolfo, Aluminum Alloys: Structure and Properties, Butterworths, London 1976.
[29] R. F. Mehl and C. S. Barrett, Trans. TMS-AIME **93**, 78 (1931).
[30] H. S. Rosenbaum and D. Turnbull, Acta metall. **7**, 664 (1959).
[31] A. H. Cottrell, Theoretical Structural Metallurgy, Edward Arnold, London 1962.
[32] J. W. Martin and R. D. Doherthy, Stability of Microstructure in Metallic Systems, Cambridge University Press, Cambridge 1976.
[33] J. Hirvonen and A. Anttila, Appl. Phys. Letters **35**, 703 (1979).
[34] B. Z. Olshanetski, S. M. Repnski, and A. A. Shklyev, Diffusion and Defect Data **23**, 27 (1980).
[35] J. C. M. Hwang, P. S. Ho, J. W. Lewis, and D. R. Campbell, J. appl. Phys. **51**, 1576 (1980).
[36] C. Laird and H. I. Aaronson, Acta metall. **17**, 505 (1969).
[37] J. E. E. Baglin, F. M. d'Heurle, and W. N. Hammer, J. appl. Phys. **50**, 226 (1979).
[38] A. Paul, J. Mater. Sci. **12**, 2246 (1977).
[39] R. G. Newton and A. Paul, Glass Technol. **21**, 307 (1980).
[40] H. I. Aaronson, H. B. Aaron, and K. R. Kinsman, Metallography **4**, 1 (1971).

(Received July 4, 1983)